

proximation, there is an additional assumption of the weak coupling ( $g^2N \ll 1$ ), and the importance of the neglected terms (of order  $g^2N$  and higher) is not known.

Experimentally, there has been some evidence<sup>24</sup> regarding the presence of spin paramagnetism in superconductors. This effect has to do with the spin density induced by a magnetic field and can be derived by means of an appropriate vertex solution. However, this does not seem to give a finite spin paramagnetism at 0°K.<sup>25</sup>

<sup>24</sup> Knight, Androes, and Hammond, *Phys. Rev.* **104**, 852 (1956); F. Reif, *Phys. Rev.* **106**, 208 (1957); G. M. Androes and W. D. Knight, *Phys. Rev. Letters* **2**, 386 (1959).

<sup>25</sup> K. Yosida, *Phys. Rev.* **110**, 769 (1958).

The collective excitations do not play an important role here as they are not excited by spin density. [ $\Gamma^{(a)}$ , Eq. (4.4), does not have the characteristic pole.]

It is desirable that both experiment and theory about spin paramagnetism be developed further since this may be a crucial test of the fundamental ideas underlying the BCS theory.

#### ACKNOWLEDGMENT

We wish to thank Dr. R. Schrieffer for extremely helpful discussions throughout the entire course of the work.

PHYSICAL REVIEW

VOLUME 117, NUMBER 3

FEBRUARY 1, 1960

### Optical Constants of Metals

MACIEJ SUFFCZYNSKI\*

*Department of Mathematics, Imperial College, London, England*

(Received August 17, 1959)

A calculation of the interband contribution to the frequency dependent dielectric constant of metals is attempted based on a specific model. The frequency region near the threshold for the interband transitions is considered. Emphasis in the model is laid on the bending of the energy bands near the Brillouin zone boundary. Attention is focused on cases when the Fermi surface approaches the zone boundary or has a finite area of contact with it. The momentum matrix element is taken as constant, which is fitted so as to achieve agreement with the experimentally found dip in the dispersion curve of the extinction coefficient. The values of the square of the matrix element for the noble metals, copper, silver, and gold, which fit the experimental data of Schulz, are found to be in the ratio 0.43:0.69:0.69.

#### 1. INTRODUCTION

THE theoretical calculation of the optical constants of metals might be interesting as there is an accumulating amount of experimental data which now becomes sufficiently consistent to allow comparison with the computed curves. Moreover the theory might indicate where further measurements of the optical constants are needed to give more information on the band structure of metals. The present knowledge of the optical properties of metals is reviewed by Givens,<sup>1</sup> Schulz,<sup>2</sup> Ginsburg and Motulevich,<sup>3</sup> and Roberts.<sup>3a</sup>

Roughly speaking in the wavelength region below  $1000 \mu$  down to  $10 \mu$  (microns) the notions of the skin effect theory are more appropriate to describe the optical properties of metals.<sup>1,4</sup> It is mainly between  $10 \mu$  and  $0.01 \mu$  where the classical concepts of the two optical constants, the refractive index  $n$  and the extinction coefficient  $k$ , apply best. In the region between  $10 \mu$  and  $1 \mu$  the simple theory of Drude is

able to predict these constants, at least the extinction coefficient, quantitatively. The refractive index predicted is always too small.

In many metals pronounced deviations from the Drude theory are observed mainly in the region of wavelengths shorter than  $1 \mu$ . These are due to the effect of the interband electronic transitions between the occupied bands and the higher empty bands. This volume effect is neglected in the classical theory of Drude. It is the purpose here to propose a simple model which would allow the calculation of the contribution of the interband transitions to the optical constants of metals.

#### 2. CLASSICAL EXPRESSIONS

The classical electromagnetic theory relates the experimentally measured refractive index  $n$  and the extinction coefficient  $k$  to the frequency dependent dielectric constant  $\epsilon(\nu)$  and the electrical conductivity  $\sigma(\nu)$ . Instead of  $\sigma$  alternatively the imaginary part of the dielectric constant may be used:  $\epsilon' = 2\sigma/\nu$

$$\begin{aligned} n &= \left\{ \frac{1}{2} [(\epsilon^2 + \epsilon'^2)^{\frac{1}{2}} + \epsilon] \right\}^{\frac{1}{2}}, \\ k &= \left\{ \frac{1}{2} [(\epsilon^2 + \epsilon'^2)^{\frac{1}{2}} - \epsilon] \right\}^{\frac{1}{2}}. \end{aligned} \quad (2.1)$$

The dielectric constant and the conductivity both consist of two parts: Drude and interband, as we shall

\* Present address: Institute of Theoretical Physics, University of Warsaw, Warsaw, Poland.

<sup>1</sup> M. P. Givens, *Solid State Physics*, edited by F. Seitz and D. Turnbull (Academic Press, Inc., New York, 1958), Vol. 6, p. 313.

<sup>2</sup> L. G. Schulz, *Suppl. Phil. Mag.* **6**, 102 (1957).

<sup>3</sup> V. L. Ginsburg and G. P. Motulevich, *Uspekhi Fiz. Nauk* **55**, 469 (1955).

<sup>3a</sup> S. Roberts, *Phys. Rev.* **100**, 1667 (1955); **114**, 104 (1959).

<sup>4</sup> R. B. Dingle, *Physica* **19**, 311, 348, 729, 1187 (1953).

shortly call them. We simply add the effect of both mechanisms

$$\epsilon = \epsilon_D + \epsilon_P, \quad \epsilon' = \epsilon_D' + \epsilon_P' \quad \text{or} \quad \sigma = \sigma_D + \sigma_P. \quad (2.2)$$

The Drude expressions,<sup>5</sup> denoted by the subscript  $D$ , are determined by the effective number of electrons per unit volume  $N$ , the static electrical conductivity  $\sigma_0$ , and the effective optical electron mass  $m^*$ . In terms of these parameters the Drude relaxation time and its reciprocal  $\gamma = e^2 N / 2\pi m^* \sigma_0$  is defined and the formulas derived:

$$\epsilon_D = 1 - Ne^2 / \pi m^* (\nu^2 + \gamma^2), \quad (2.3)$$

$$\sigma_D = \gamma^2 \sigma_0 / (\nu^2 + \gamma^2). \quad (2.4)$$

For frequencies  $\nu$  sufficiently large to neglect  $\gamma$  the imaginary part of the Drude dielectric constant is negligibly small and the real part gives the usual contribution due to the acceleration of the electrons with the effective mass  $m^*$ .

### 3. THE INTERBAND TRANSITIONS

The calculation of the interband electronic transitions in solids has been done by Kronig.<sup>6,7</sup> Later an improved treatment based on the nearly free electron approximation has been given by Sergeiev and Tchernikovskiy<sup>8</sup> and their formulas persist until today in the literature.<sup>5,9-11</sup> For this formulation of the theory it is necessary to assume that the Fermi surface does not touch the Brillouin zone boundary. If it does the matrix elements become infinite.

The theory of the interband transitions for insulators has been developed by Wilson.<sup>9</sup> He noticed the peculiar form of the dispersion curve resulting from the interband transitions between the filled bands.

The terms which the interband transitions contribute to the dielectric constant and the conductivity will be calculated according to the standard formulas.<sup>5,12</sup> The local field corrections<sup>13</sup> are neglected. Fermi distribution function is taken at the absolute zero.

The formula for the real part of the dielectric constant will be used in the form which utilizes the  $f$ -sum rule. This makes possible the separation of the contribution from the conduction electrons which is already taken into account by the Drude term, Eq. (2.3).

Therefore the real part of the interband dielectric

constant is the principal value of

$$\epsilon_P = \frac{e^2}{\pi m^2 h} \frac{2}{(2\pi)^3} \frac{2}{3} \sum_{s'} \sum_s \int \frac{|\mathbf{P}_{s's}|^2 d^3 k}{\nu_{s's}(\nu_{s's}^2 - \nu^2)}, \quad (3.1)$$

and the imaginary part is

$$\epsilon_P' = \frac{e^2}{2m^2 h \nu^2} \frac{2}{(2\pi)^3} \frac{2}{3} \sum_{s'} \sum_s \int |\mathbf{P}_{s's}|^2 \delta(\nu_{s's} - \nu) d^3 k. \quad (3.2)$$

Here  $m$  is the ordinary electron mass,  $h\nu_{s's} = E_{s'} - E_s$  is the energy difference between band  $s'$  and  $s$ . The momentum of the incident electromagnetic radiation of frequency  $\nu$  is neglected, thus the electronic transitions are vertical only, in the reduced zone scheme. The summation of the wave vector  $\mathbf{k}$  goes therefore over such states that are occupied by electrons in the band  $s$  and unoccupied in band  $s'$ . The matrix element of the interband transitions

$$\mathbf{P}_{s's}(\mathbf{k}) = -\frac{\hbar}{i} \int \mathbf{u}_{s'\mathbf{k}}^* \nabla \mathbf{u}_{s\mathbf{k}} d^3 x \quad (3.3)$$

is a quantity which is difficult to evaluate. There are arguments that the absolute value of it should decrease away from the zone boundary towards the zone center, especially when the symmetry types of the lower and upper bands differ at the zone boundary, being there purely  $s$  like and  $p$  like, respectively.<sup>14,15</sup> For the present we limit our calculation taking the matrix element constant. The values of the constant will be determined, whenever possible, from comparison with the experimentally known dispersion curves (Sec. 5).

### 4. BAND MODEL

To enable explicit analytical calculations we are looking for a simple model which would contain in a natural way the relevant quantities characteristic for the bands involved, such as the band separation, the Fermi level, etc.

There has recently been much discussion as to whether the Fermi surface does or does not touch the boundary of the Brillouin zone, particularly in the noble metals. The question is of a fundamental nature as the difference between a singly connected and multiply connected Fermi surface should have its bearing on many electronic properties which depend on the density of states and band anisotropy. A few properties like the thermoelectric power,<sup>16</sup> the electronic specific heat,<sup>17</sup> magnetoresistance,<sup>18</sup> and the anomalous

<sup>5</sup> A. H. Wilson, *The Theory of Metals* (Cambridge University Press, New York, 1936).

<sup>6</sup> R. L. Kronig, Proc. Roy. Soc. (London) **A124**, 406 (1929); Proc. Roy. Soc. (London) **A133**, 255 (1931).

<sup>7</sup> H. Y. Fan, Phys. Rev. **68**, 43 (1945).

<sup>8</sup> M. I. Sergeiev and M. G. Tchernikovskiy, Physik Z. Sowjetunion **5**, 106 (1934).

<sup>9</sup> A. H. Wilson, Proc. Roy. Soc. (London) **A151**, 274 (1935).

<sup>10</sup> P. N. Butcher, Proc. Phys. Soc. (London) **A64**, 765 (1951).

<sup>11</sup> E. M. Baroody, Phys. Rev. **101**, 1679 (1956).

<sup>12</sup> F. Seitz, *The Modern Theory of Solids* (McGraw-Hill Book Company, Inc., New York, 1940), pp. 649 ff.

<sup>13</sup> See the series of papers: P. Nozières and D. Pines, Phys. Rev. **109**, 741, 762, 778 (1958); **113**, 1254 (1959); J. Hubbard, Proc. Phys. Soc. (London) **A68**, 441, 976 (1955).

<sup>14</sup> N. F. Mott and H. Jones, *Theory of the Properties of Metals and Alloys* (Oxford University Press, New York, 1936).

<sup>15</sup> M. H. Cohen and V. Heine, *Advances in Physics*, edited by N. F. Mott (Taylor and Francis, Ltd., London, 1958), Vol. 7, p. 395.

<sup>16</sup> H. Jones, Proc. Phys. Soc. (London) **A68**, 1191 (1955).

<sup>17</sup> H. Jones, Proc. Roy. Soc. (London) **A240**, 321 (1957).

<sup>18</sup> R. Olsen and S. Rodriguez, Phys. Rev. **108**, 1212 (1957).

skin effect<sup>19</sup> may be mentioned at once and many others can be found in literature.<sup>20-23</sup>

We would like to set up a model which would allow the calculation of the optical constants, taking into account the details which are important near the zone boundary. That is, the energy gap, the bending of the energy bands, and the Fermi surface which approaches the zone boundary closely or eventually touches it, even with a finite area of contact. There is a variety of possibilities amenable to analytical calculation. We limit our discussion to a particular one.

We assume the two bands  $E_+$  and  $E_-$  of the following dependence on the wave vector  $k_x, k_y, k_z$

$$E_{\pm}(k_x, k_y, k_z) = \frac{\hbar^2}{2} \left\{ \frac{1}{m_{T\pm}} (k_x^2 + k_y^2) + \frac{1}{m_L} [k_L^2 + (k_z - k_L)^2] \pm 2k_L [(k_z - k_L)^2 + V_L^2]^{\frac{1}{2}} \right\}. \quad (4.1)$$

In the noble metals nearest to the Fermi surface are the hexagonal faces of the Brillouin zone. We put therefore the  $k_z$  axis along the  $\Gamma L$  line in  $\mathbf{k}$  space and take  $k_L$  equal to the length  $\Gamma L$ . The form of the energy bands is closely similar to the one obtained from the nearly free electron approximation,<sup>24</sup> but we take the transverse effective masses  $m_{T+}$  and  $m_{T-}$  in the two bands to be different, in general. The energy bands

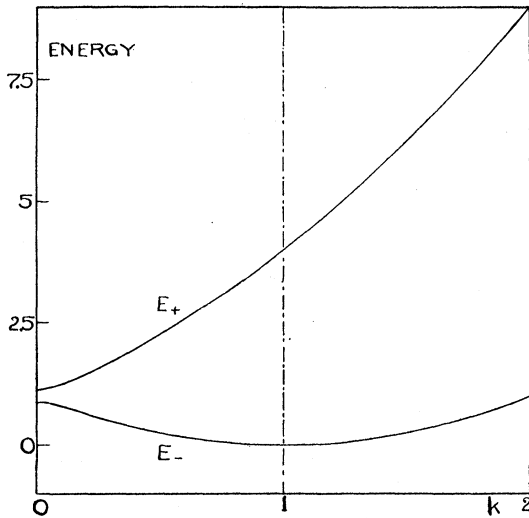


FIG. 1. Energy bands in copper according to Eq. (4.1). The cross section is along the  $\Gamma L$  line. The energy gap at the point  $L$  is 2.25 eV.

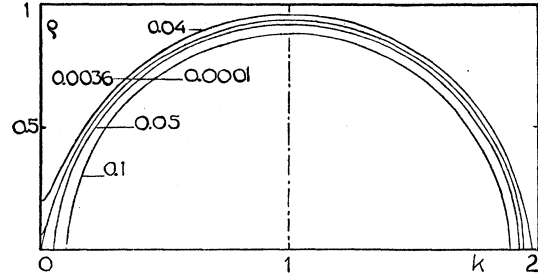


FIG. 2. Fermi surfaces in copper according to Eq. (4.9) and (4.19). The cross section is along the  $\Gamma L$  line. The parameters are in succession  $k_1 = 0.1, 0.05, 0.0001$ , and  $a = 0.0036, 0.04$ .

have the axial symmetry along the  $\Gamma L$  axis, the cross section is shown in Fig. 1. The constant  $2\hbar^2 k_L V_L / m_L$  is the energy gap at the point  $L$ .

The occupied states in the lower band are bounded by the surface  $E_-(k_x, k_y, k_z) = E_F$ , where the constant  $E_F$  has the meaning of the Fermi energy.<sup>25</sup> The examples of the Fermi surfaces are shown in cross section in Fig. 2.

The energy difference between the two bands (4.1) is

$$E_+ - E_- = \hbar^2 \left\{ \frac{1}{2} \left( \frac{1}{m_{T+}} - \frac{1}{m_{T-}} \right) (k_x^2 + k_y^2) + \frac{2}{m_L} k_L [(k_L - k_z)^2 + V_L^2]^{\frac{1}{2}} \right\}. \quad (4.2)$$

We introduce the dimensionless parameters

$$\alpha = \frac{m}{2} \left( \frac{1}{m_{T+}} - \frac{1}{m_{T-}} \right), \quad (4.3)$$

$$\rho = (k_x^2 + k_y^2)^{\frac{1}{2}} / k_L, \quad k = (k_L - k_z) / k_L, \quad V = V_L / k_L. \quad (4.4)$$

Thus for the point  $\Gamma$  or (000) we have  $\rho = 0, k = 1$ , for the point  $L$  or  $(00k_L)$  we have  $\rho = 0, k = 0$ . We put for simplicity  $m_L = m_{T+} = m$ , and we take  $\alpha$  positive. Further we abbreviate

$$\phi = 2mE_F(\hbar k_L)^{-2}, \quad (4.5)$$

$$\sigma = \frac{\pi m \nu}{\hbar k_L^2} = \frac{2\pi^2 m c}{k_L^2 \hbar \lambda}, \quad (4.6)$$

$$M = \frac{e^2 m}{3\hbar^4} \frac{|\mathbf{P}_{+-}|^2}{4\pi k_L^3} = \frac{1}{3} \frac{|\mathbf{P}_{+-}|^2 / (\hbar k_L)^2}{4\pi a_B k_L}. \quad (4.7)$$

The abbreviations  $k$  in (4.4) and  $\sigma$  in (4.6) should not be confused with the standard symbols in Eqs. (2.1).  $\lambda$  is the wavelength,  $c$  is the velocity of light and  $a_B$  is the Bohr radius.

<sup>25</sup> I am indebted to Professor H. Jones for the suggestion on the Fermi surface.

<sup>19</sup> A. B. Pippard, Phil. Trans. Roy. Soc. London A250, 325 (1957).

<sup>20</sup> V. Heine, Proc. Roy. Soc. (London) A240, 340 (1957).

<sup>21</sup> M. H. Cohen, Phil. Mag. 49, 762 (1958).

<sup>22</sup> F. Garcia-Moliner, Proc. Phys. Soc. (London) 72, 996 (1958); J. M. Ziman, Phil. Mag. 4, 371 (1959).

<sup>23</sup> W. Kohn, Phys. Rev. Letters 2, 393 (1959).

<sup>24</sup> R. Peierls, Ann. Physik 4, 121 (1930); H. Jones, Proc. Phys. Soc. (London) A49, 250 (1937).

## (a) Multiply-Connected Fermi Surface

If the Fermi surface touches the Brillouin zone boundary we can characterize it in our model by the area of contact with the boundary plane. We write  $a = [\rho_F(k=0)]^2$ , and have from (4.1)

$$a = \phi - 1 + 2V. \quad (4.8)$$

The integration in (3.1, 2) must extend over  $\rho$  from 0 to the upper limit  $\rho_F(k)$  given by

$$[\rho_F(k)]^2 = \phi - 1 - k^2 + 2(k^2 + V^2)^{\frac{1}{2}}, \quad (4.9)$$

and over  $k$  from 0 to  $k_2$ . There are two possibilities of choice for  $k_2$ . If we require the energy bands to be symmetric with respect to the reflection in the  $k_z=0$  plane, we have to integrate between  $k_z=k_L$  and  $k_z=0$ .

The calculated expressions for the dielectric constant then have discontinuity in slope for the frequency corresponding to the band separations at  $k_z=0$ . For frequencies not greatly exceeding the energy gap at  $L$  the expressions are as good as in the second model in which we integrate from  $k_z=k_L$  not only to  $k_z=0$  but further to  $k_z=-k_L$ . The bands in this second model are not exactly symmetric with respect to reflection in  $k_z=0$  plane (see Fig. 1), but the dielectric constant expressions do not suffer discontinuity in slope for the aforementioned frequency. We are interested in the optical region which extends a few electron volts on both sides of the energy gap; the differences between the results of calculations based on either model are completely negligible. We usually integrate down to  $k_z=0$ , i.e., our  $k_2=1$ .

Using our abbreviations we have

$$\epsilon_P = 16M \int_0^{k_2} dk \int_0^{\rho_F(k)} \rho d\rho \{ [\alpha\rho^2 + 2(k^2 + V^2)^{\frac{1}{2}}] [(\alpha\rho^2 + 2(k^2 + V^2)^{\frac{1}{2}})^2 - (2\sigma)^2] \}^{-1}, \quad (4.10)$$

$$\epsilon_P' = 2\pi \frac{M}{\sigma^2} \int_0^{k_2} dk \int_0^{\rho_F(k)} \rho d\rho \delta[\alpha\rho^2 + 2(k^2 + V^2)^{\frac{1}{2}} - 2\sigma]. \quad (4.11)$$

The result of the integration (4.10) can be written

$$\epsilon_P = \frac{M}{\alpha\sigma^2} \left\{ k_2 \ln \left| \frac{(k_2^2 + V^2)[(2(1+1/\alpha)(k_2^2 + V^2)^{\frac{1}{2}} - k_2^2 + \phi - 1)^2 - (2\sigma/\alpha)^2]}{(k_2^2 + V^2 - \sigma^2)(2(1+1/\alpha)(k_2^2 + V^2)^{\frac{1}{2}} - k_2^2 + \phi - 1)^2} \right| \right. \\ \left. + \sum_{i=0}^2 [A_i(\sigma, k_2) + A_i(-\sigma, k_2) - 2A_i(0, k_2)] \right\}, \quad (4.12)$$

where

$$A_0(\sigma, k) = -(V^2 - \sigma^2)^{\frac{1}{2}} \arctan[k(V^2 - \sigma^2)^{-\frac{1}{2}}] \text{ for } |\sigma| < V \\ = -\frac{1}{2}(\sigma^2 - V^2)^{\frac{1}{2}} \ln \left| \frac{k + (\sigma^2 - V^2)^{\frac{1}{2}}}{k - (\sigma^2 - V^2)^{\frac{1}{2}}} \right| \text{ for } |\sigma| > V. \quad (4.13)$$

For  $i=1, 2$

$$A_i(\sigma, k) = [V^2 - s_i^2(\sigma)]^{\frac{1}{2}} \{ \arctan[k(V^2 - s_i^2(\sigma))^{-\frac{1}{2}}] + \arctan[ks_i(\sigma)[(k^2 + V^2)(V^2 - s_i^2(\sigma))]^{-\frac{1}{2}} \} \text{ for } |s_i(\sigma)| < V \\ = [s_i^2(\sigma) - V^2]^{\frac{1}{2}} \ln \left| \frac{ks_i(\sigma) + \{(k^2 + V^2)[s_i^2(\sigma) - V^2]\}^{\frac{1}{2}}}{V\{k - [s_i^2(\sigma) - V^2]^{\frac{1}{2}}\}} \right| \text{ for } |s_i(\sigma)| > V. \quad (4.14)$$

Here

$$s_i(\sigma) = (1+1/\alpha) \mp [(1+1/\alpha)^2 + V^2 + \phi - 1 - 2\sigma/\alpha]^{\frac{1}{2}}. \quad (4.15)$$

For  $i=1$  the  $-$  sign and for  $i=2$  the  $+$  sign is taken.

The imaginary part of the dielectric constant can be calculated as done by Wilson<sup>9</sup> and Dexter.<sup>26</sup> It is proportional to the difference between the  $k$  values of the intersection of the curve  $\alpha\rho^2 + 2(k^2 + V^2)^{\frac{1}{2}} - 2\sigma = 0$  with the boundaries of the  $\rho, k$  region of integration.

For frequencies below the threshold for the photo-

electric absorption,  $\sigma = V$ , the imaginary part vanishes. For frequencies between

$$V < \sigma < V + \alpha\alpha/2, \quad \epsilon_P' = (\pi M/\alpha\sigma^2)(\sigma^2 - V^2)^{\frac{1}{2}}. \quad (4.16)$$

For frequencies

$$V + \alpha\alpha/2 < \sigma < (k_2^2 + V^2)^{\frac{1}{2}}, \\ \epsilon_P' = (\pi M/\alpha\sigma^2) \{ (\sigma^2 - V^2)^{\frac{1}{2}} - [s_i^2(\sigma) - V^2]^{\frac{1}{2}} \}. \quad (4.17)$$

Frequencies still higher are not interesting as for most metals they lie in the ultraviolet.

The real part of the dielectric constant has a maximum at the frequency  $\sigma = V$ . If the difference between

<sup>26</sup> D. L. Dexter, *Proceedings of the Conference on Photoconductivity, Atlantic City, 1954*, edited by R. G. Breckenridge et al. (John Wiley and Sons, Inc., New York, 1956), p. 155.

the transverse effective masses in the two bands is small the height of this maximum is proportional to  $(a/\alpha)^{1/2}$ .

The imaginary part has the maximum at the higher frequency  $\sigma = V + a\alpha/2$ . It is also proportional to  $(a/\alpha)^{1/2}$ , its width being proportional to  $a\alpha$ . The frequency derivative of the real and imaginary part is discontinuous at these maxima. It is necessary to have the transverse effective masses  $m_{T+}$  and  $m_{T-}$  slightly different, that is  $\alpha \neq 0$ , in order to keep the real and imaginary part finite at the maxima. Discussion of the effect of the transverse effective masses for the calculation of the optical absorption can be found in reference 9 and particularly in reference 26.

### (b) Singly-Connected Fermi Surface

The case where the Fermi surface does not touch the Brillouin zone boundary can be dealt with using essentially the same formulas. The Fermi surface can now be characterized by its distance from the point  $L$ , call it  $k_1$ ,

$$\phi = k_1^2 + 1 - 2(k_1^2 + V^2)^{1/2}. \quad (4.18)$$

$$\epsilon_P = M \left\{ [k_1^2 + V^2 - 2(k_1^2 + V^2)^{1/2} - \sigma^2] [B(\sigma, k_2) - B(\sigma, k_1)] + 2[B_0(\sigma, k_2) - B_0(\sigma, k_1)] + \ln \left( \frac{k_1 + (k_1^2 + V^2)^{1/2}}{k_2 + (k_2^2 + V^2)^{1/2}} \right) \right\}. \quad (4.22)$$

Here

$$\begin{aligned} B(\sigma, k) &= (1/\sigma)(V^2 - \sigma^2)^{-1/2} \arctan[k\sigma[(k^2 + V^2)(V^2 - \sigma^2)]^{-1/2}] \quad \text{for } \sigma < V \\ &= (1/2\sigma)(\sigma^2 - V^2)^{-1/2} \ln \left| \frac{k\sigma - [(k^2 + V^2)(\sigma^2 - V^2)]^{1/2}}{k\sigma + [(k^2 + V^2)(\sigma^2 - V^2)]^{1/2}} \right| \quad \text{for } \sigma > V, \end{aligned} \quad (4.23)$$

$$\begin{aligned} B_0(\sigma, k) &= (V^2 - \sigma^2)^{-1/2} \arctan[k(V^2 - \sigma^2)^{-1/2}] \quad \text{for } \sigma < V \\ &= \frac{1}{2}(\sigma^2 - V^2)^{-1/2} \ln \left| \frac{k - (\sigma^2 - V^2)^{1/2}}{k + (\sigma^2 - V^2)^{1/2}} \right| \quad \text{for } \sigma > V. \end{aligned} \quad (4.24)$$

The imaginary part is now, for  $\sigma > (k_1^2 + V^2)^{1/2}$ ,

$$\epsilon_P' = (\pi M/\sigma)(\sigma^2 - V^2)^{-1/2} [k_1^2 + V^2 - 2(k_1^2 + V^2)^{1/2} - \sigma^2 + 2\sigma]. \quad (4.25)$$

The formulas (4.22, 25) are obtained more simply by first setting  $\alpha = 0$  in (4.10, 11) and then integrating. For Fermi surfaces without contact only these simpler formulas (4.22) and (4.25) were used in numerical computations, with however one modification. The model we are aiming at should simulate as much as possible the actual shape of bands in the metal. The energy bands assumed do not comply with the symmetry requirements of the fcc lattice, they are only axially symmetric along  $\Gamma L$  line. There are eight hexagonal faces in the actual Brillouin zone. To simulate this situation the following refinement has been used for the case of Fermi surfaces with no contact. The dielectric constant has been calculated first with the limits of integration  $k = k_1$  and  $k = k_2$ , call it  $\epsilon_P(k_1, k_2)$ , then with the limits  $k = 0.1$  and  $k = k_2$ , call it  $\epsilon_P(0.1, k_2)$ .

The Fermi surface equation can be written

$$[\rho_F(k)]^2 = k_1^2 - 2(k_1^2 + V^2)^{1/2} - k^2 + 2(k^2 + V^2)^{1/2}. \quad (4.19)$$

The real part of the dielectric constant is now expressible as the difference

$$\epsilon_P(k_1, k_2) = \epsilon_P(k_2) - \epsilon_P(k_1), \quad (4.20)$$

where  $\epsilon_P(k)$  for  $k = k_2$  is written down in (4.12). The imaginary part now has the threshold at the frequency  $\sigma = (k_1^2 + V^2)^{1/2}$ . For the frequency range

$$\begin{aligned} (k_1^2 + V^2)^{1/2} &< \sigma < (k_2^2 + V^2)^{1/2}, \\ \epsilon_P' &= (\pi M/\alpha\sigma^2) \{ (\sigma^2 - V^2)^{1/2} - [s_1^2(\sigma) - V^2]^{1/2} \}. \end{aligned} \quad (4.21)$$

When the Fermi surface has no finite area of contact with the zone boundary one can take the limiting case of small  $\alpha$  and the real and imaginary part of the dielectric constant remain, even for  $\alpha = 0$ , continuous at the threshold frequency. Taking  $\alpha$  small, developing the square roots and keeping only terms of the first power in  $\alpha$  which cancel with the  $\alpha$  in the denominator before the curly bracket in (4.12) one obtains from (4.20)

In the fcc metal the distance between the hexagonal face of the Brillouin zone and the Fermi sphere for one electron per atom is  $0.0975k_L$ . The actual real and imaginary parts of the dielectric constant used were calculated as

$$\epsilon_P = \frac{1}{4} \{ 4[\epsilon_P(k_1, k_2) - \epsilon_P(0.1, k_2)] + \epsilon_P(0.1, k_2) \}, \quad (4.26)$$

to simulate the effect of the four pairs of hexagonal faces. It must be said that this refinement which numerically was rather small was not being done for surfaces with a finite area of contact because then the formulas were used with  $\alpha \neq 0$  and these are very lengthy. The comparison of the numerical results obtained in the two different cases, contact and no contact, must be taken with due reserve.

We mention another circumstance about the Fermi surfaces without contact, i.e., simply connected. When such a surface recedes further away from the Brillouin zone boundary the maximum in the real part of the dielectric constant gets shifted to higher frequency than

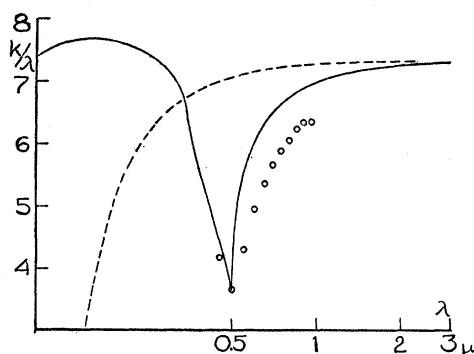


FIG. 3. The calculated values of  $k/\lambda$  vs  $\ln\lambda$  for gold. The solid curve was computed with  $k_1=0.01$ ,  $M=0.72$ . The broken curve was computed from the Drude formulas. The circles denote the experimental points of Schulz.

the one corresponding to the energy gap at the point  $L$ . To adjust the position of the maximum to the experimentally given frequency one has to choose the value of  $V$  smaller than the energy gap at the point  $L$ .

The contact of the Fermi surface with the zone boundary has a pronounced effect on the resulting dispersion curve. As already remarked a finite area of contact gives rise to the sharp, narrow peak in the imaginary part of the dielectric constant, at a frequency higher by  $\alpha a/2$  than the threshold frequency. This peak does not exist for Fermi surfaces without finite area of contact.

When the extinction coefficient dispersion curves are calculated with reasonable values of the constant  $M$ , see Sec. 5, it is apparent that, for surfaces with contact, the aforementioned peak of the imaginary part does not exhibit itself very strongly, especially when  $a$  is small and  $\alpha$  is not. It may be that the experimental curves are not at all sufficiently precise or the peaks in them are spread out by different factors, like the phonon scattering, nonvertical transitions, and temperature, polycrystalline, and surface effects, etc. Eventually the sharp narrow peak in the immediate vicinity of the threshold for the internal photoelectric absorption can be undetectable.

On the other hand, the peak in the real part of the dielectric constant exists, in every case, whenever the Fermi surface approaches closely the zone boundary, irrespective of whether contact is achieved or not. Therefore the conclusion whether the Fermi surface

TABLE I. The Drude parameters adopted for the calculation of the dispersion curves. The wavelength  $\lambda$  in microns is given at which the dip in the experimental  $k/\lambda$  curve is centered.  $N$  is the effective number of electrons in  $10^{22} \text{ cm}^{-3}$ ,  $\sigma_0$  is the static electrical conductivity in  $10^{17} \text{ sec}^{-1}$ ,  $m^*$  is the effective optical electron mass.

	$N$	$\sigma_0$	$m^*$	$\lambda$
Copper	8.5	5.76	1.45	0.55
Silver	5.9	5.55	0.97	0.325
Gold	5.9	4.2	0.98	0.5

does or does not touch the Brillouin zone boundary is difficult to draw. The peak in the real part of the dielectric constant is due to the increased density of states near the zone boundary. In the present treatment, with the matrix element constant, the density of states is the only determining factor. The increased density of states is ultimately connected with the energy gap at the boundary plane.

The situation is similar with every energy gap, and it should be similar in a superconductor where the energy gap exists in the microwave region of frequencies.<sup>27-29</sup>

### (c) The $d$ Band

Until now only one filled and one unoccupied band have been considered, all other bands being disregarded. There are indications<sup>14,30</sup> that in copper the transitions from the filled  $3d$  band also contribute to the anomalies in the dispersion curve. It was therefore attempted to calculate the contributions from a tentatively described

TABLE II. The relative magnitudes of the squared matrix element for the interband transitions, as used in the calculations for the noble metals. The Fermi surface was assumed to approach the zone boundary by the distance  $k_1$ .

$k_1 =$	0.05	$10^{-2}$	$10^{-3}$	$10^{-4}$	$10^{-5}$
Copper	0.64	0.45	0.44	0.43	0.43
Silver	1.0	0.7	0.69	0.69	0.69
Gold	0.94	0.72	0.7	0.69	0.69

$d$  band. The  $d$  band was assumed in the form

$$E = E_0 + \frac{\hbar^2}{2m_{Td}}(k_x^2 + k_y^2) + \frac{\hbar^2}{2m_{Ld}}\{k_L^2 + (k_z - k_L)^2 - 2k_L[(k_z - k_L)^2 + V_L^2]^{\frac{1}{2}}\}. \quad (4.27)$$

The  $3d$  band in copper is completely filled. For simplicity the filled zone has been approximated by a cylinder of length  $k_L$  and of radius  $\rho_L k_L$  corresponding to the circle inscribed into the hexagonal face of the Brillouin zone. The transitions were considered to the band  $E_+$  of Eq. (4.1), with a constant matrix element. Its square was taken proportional to the parameter  $M_d$ . The calculation proceeds similarly to the previous case of the Fermi surface with contact. The area of contact is now very big. It is essential to have the transverse effective masses  $m_{Td}$  and  $m_{T+}$  different.<sup>26</sup> The disposable constants which we now have in addition are (1) the width of the  $d$  band,  $W_d = E(00k_L) - E_0$ , (2) its minimum separation from the unoccupied band  $E_+$ , i.e.,

<sup>27</sup> R. H. Glover and M. Tinkham, Phys. Rev. **108**, 243 (1957).

<sup>28</sup> D. C. Mattis and J. Bardeen, Phys. Rev. **111**, 412 (1958).

<sup>29</sup> Biondi, Forrester, Garfunkel, and Satterthwaite, Revs. Modern Phys. **30**, 1109 (1958); P. L. Richards and M. Tinkham, Phys. Rev. Letters **1**, 318 (1958); Ginsberg, Richards, and Tinkham, Phys. Rev. Letters **3**, 337 (1959).

<sup>30</sup> J. Friedel, Proc. Phys. Soc. (London) **B65**, 769 (1952).

the energy gap at the point  $L$ ,  $U_d = E_+(00k_L) - E(00k_L)$ , (3) the area,  $a_d = \rho_L^2$ , and (4) the difference

$$\alpha_d = \frac{m}{2} \left( \frac{1}{m_{T+}} - \frac{1}{m_{Td}} \right). \quad (4.28)$$

## 5. COMPARISON WITH EXPERIMENTAL DATA

### (a) Noble Metals

For the wavelengths between  $3\mu$  and  $0.25\mu$  the experimental curves of the extinction coefficient taken recently by Schulz<sup>2,31</sup> can serve as a basis for comparison. Schulz plotted  $k/\lambda$  versus  $\ln\lambda$  (Fig. 3). We have used Schulz's values for the parameters  $N$ ,  $\sigma_0$ , and  $m^*$  in the calculation of the Drude contributions, see Table I. For wavelengths longer than  $1\mu$  the agreement between the experiment and the calculated Drude values is generally good for the extinction coefficient. However

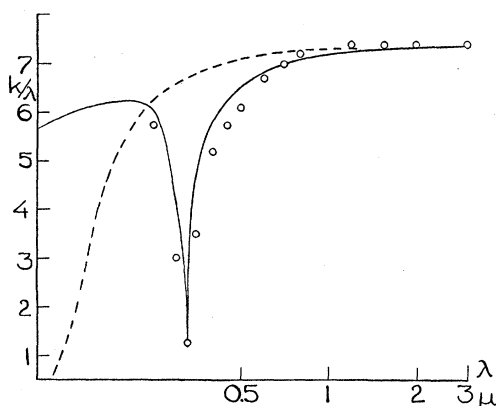


FIG. 4. The calculated values of  $k/\lambda$  vs  $\ln\lambda$  for silver. The solid curve was computed with  $k_1=0.0001$ ,  $M=0.69$ . The broken curve was computed from the Drude formulas. The circles denote the experimental points of Schulz.

the refractive index calculated from Drude formulas is several times too small and the addition of the interband contributions does not improve it satisfactorily. (See Figs. 3–7.)

The noble metals exhibit departures from the simple Drude theory in the form of well shaped dips in the  $k/\lambda$  curves.<sup>2</sup> These can be reproduced by the present theory reasonably well. The wavelength (see Table I) at which the dip is centered was, as explained earlier, determining the value of the energy gap  $V$ . The value of the  $k_L$  is determined by the lattice constant  $a_0$ , in the fcc metal  $k_L = \pi\sqrt{3}/a_0$ . The interband contribution was calculated for the different Fermi surfaces approaching the zone boundary by distance  $k_1$ . For each  $k_1$  the constant  $M$  was chosen so that in the dispersion curve of  $k/\lambda$  the resulting dip reproduces as closely as possible the one found experimentally.

The portion of the dispersion curve for wavelengths

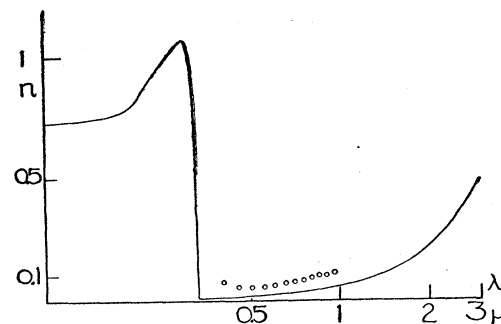


FIG. 5. The calculated values of the refractive index  $n$  vs  $\ln\lambda$  for silver, with the same parameters as used in Fig. 4. The circles denote the experimental points of Schulz.

longer than  $1\mu$  was not sensitive to the choice of  $M$ , but the computed curve was dependent critically on  $M$  for short wavelengths.

The case when the Fermi surface just touches the Brillouin zone boundary, that is  $k_1=0$ , has been discussed elsewhere.<sup>32</sup>

Proceeding from lighter to heavier noble metals it was found necessary to take the constant  $M$ , for the given  $k_1$  value, larger for silver and gold than for copper, see Table II. This shows a reasonable trend in the values of the optical matrix element, as can be expected when we imagine it calculated between the orthogonalized plane waves.<sup>21,33</sup> The fact that the optical constants of metals vary in a regular way with the atomic number has been noticed by Nathanson.<sup>34</sup>

It is seen from Figs. 4 and 6 that the dip in the calculated  $k/\lambda$  curve is narrower if the spread in the energy bands involved, see Fig. 1, is smaller. For silver the energy of the free electron at the point  $L$  is 6.76 eV higher than at the point  $\Gamma$  and the energy gap at  $L$  was taken as 3.81 eV, the ratio is thus 1.77. The dip in the  $k/\lambda$  curve is too narrow. For copper the free electron energy at  $L$  is 8.67 eV, the energy gap at  $L$  was taken as 2.25 eV, the ratio is 3.85, and the dip in the  $k/\lambda$  curve, computed with no contact, is too broad.

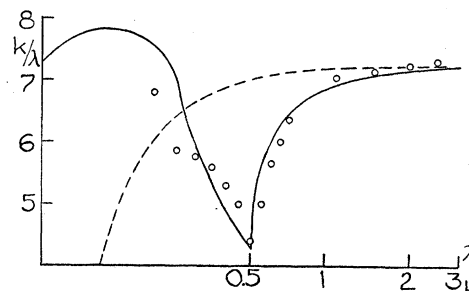


FIG. 6. The calculated values of  $k/\lambda$  vs  $\ln\lambda$  for copper. The solid curve was computed with  $k_1=0.0001$ ,  $M=0.444$ . The broken curve was computed from the Drude formulas. The circles denote the experimental points of Schulz.

<sup>32</sup> M. Suffczynski, Proc. Phys. Soc. (London) **73**, 671 (1959).

<sup>33</sup> M. Suffczynski, Bull. acad. polon. sci. **6**, 481 (1958).

<sup>34</sup> J. B. Nathanson, J. Opt. Soc. Am. **28**, 300 (1938).

<sup>31</sup> L. G. Schulz, J. Opt. Soc. Am. **44**, 357 (1954).

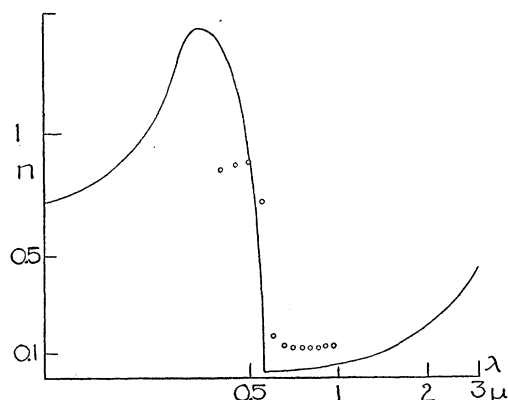


FIG. 7. The calculated values of the refractive index  $n$  vs  $\ln\lambda$  for copper, with the same parameters as used in Fig. 6. The circles denote the experimental points of Schulz.

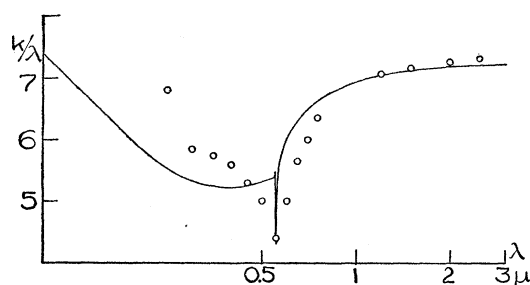


FIG. 8. The calculated values of  $k/\lambda$  vs  $\ln\lambda$  for copper. The curve was computed with the Fermi surface having the contact with the zone boundary. The value of  $a=0.001$ ,  $\alpha=0.25$ ,  $M=0.29$ .

The calculations with the matrix element not constant, but diminishing in the absolute value away from the zone boundary towards the zone center, made the resulting dip narrower.

For copper, which has a complicated shape of the dip in  $k/\lambda$  curve, the calculations have been done for the case of the Fermi surface with a finite area of contact. It is realized that it is difficult to reconcile, in principle, the small energy gap (2.25 eV) with the contact at the zone boundary; very strong anisotropy of the Fermi surface would be required. Two examples of the curves computed from the formulas (4.12-17), for particular choice of the parameters, are shown in Figs. 8 and 9.

For copper, also, the calculation has been tried with the contribution from the  $d$  band. An example of the curve obtained is given in Fig. 10.

#### (b) Other Metals

A few remarks now concerning other than noble metals.

For zinc, the one divalent metal for which many optical measurements have been reported,<sup>1,2</sup> the comparison with the experimental points presents difficulties because of lack of agreement between the

different experimenters, as is seen from the graphs quoted by Schulz.<sup>2</sup> The Drude parameters envisaged for zinc by different workers are widely different.<sup>2,35</sup> On the other hand Givens<sup>1</sup> has plotted the dielectric constant and the conductivity of several metals *versus* wavelength in the two-way-logarithmic scale. For zinc, according to measurements of Bor *et al.*<sup>36</sup>  $\epsilon$  exhibits a sharp peak for  $\lambda \approx 1 \mu$ , and  $\sigma$  has a broad peak for  $\lambda \lesssim 1$ . This is in line with the theoretical arguments for zinc that the Fermi surface touches the planes bounding a zone containing two electrons per atom<sup>5</sup> or an overlap takes place. It is possible in zinc that peaks in the density of states arise at two different energies, which renders a more complicated situation in the optical properties. It would be very valuable to repeat with an improved accuracy the optical measurements on zinc and copper-zinc alloys. The tentatively computed  $k/\lambda$  curve for zinc reproduces the results of reference 36 only qualitatively, see Fig. 11. It was difficult to find reasonable values of parameters to fit the experimental points, see Table III. Similar to zinc are the experi-

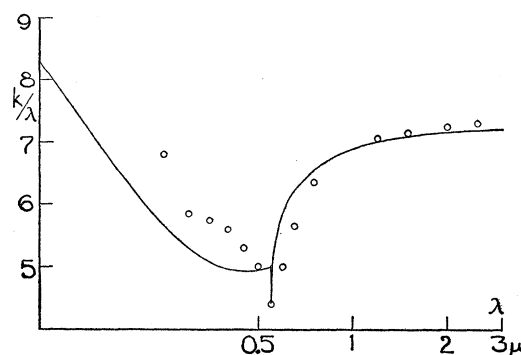


FIG. 9. The calculated values of  $k/\lambda$  vs  $\ln\lambda$  for copper. The curve was computed with the Fermi surface having the contact with the zone boundary. The value of  $a=0.0001$ ,  $\alpha=0.1225$ ,  $M=0.3163$ .

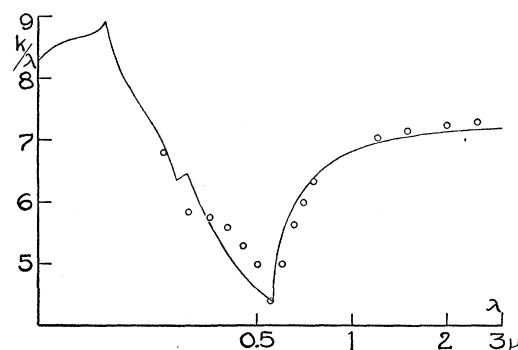


FIG. 10. The calculated values of  $k/\lambda$  vs  $\ln\lambda$  for copper. The curve was computed with  $k_1=0.001$ ,  $M=0.41$ . The  $d$ -band contribution was added with  $a_d=0.5$ ,  $W_d=5.2$  eV,  $U_d=4.5$  eV,  $\alpha_d=0.36$ ,  $M_d=0.034$ .

<sup>35</sup> J. N. Hodgson, Proc. Phys. Soc. (London) **B68**, 593 (1955).

<sup>36</sup> Bor, Hobson, and Wood, Proc. Phys. Soc. (London) **51**, 932 (1939).



mental dispersion curves for beryllium<sup>1</sup> though the peaks are much broader there.

In the dispersion curve for aluminium no well-shaped dip can be found. The overlap into the second zone does take place in aluminium,<sup>20</sup> but probably to such a considerable extent that, due to the selection rule of the vertical transitions, the states near the energy gap cannot play a role. The upper band near the zone boundary may be occupied by the overlapping electrons.

We do not discuss the alkali metals as they are usually dealt with in the standard form of the theory as proposed by Sergeiev and Tchernikovskiy.<sup>8-10</sup> Since the alkali metals have the bcc structure and the Fermi surface probably remains nearly spherical, the energy gap plays no essential role in the calculation of the optical constants for these metals.

There are serious theoretical indications,<sup>21,22</sup> however, that in lithium the Fermi surface is strongly anisotropic and actually does touch the zone boundary. We have purely tentatively computed the  $k/\lambda$  curves for lithium assuming a small area of contact and a rather small matrix element, see Fig. 12. The energy gap was taken<sup>37</sup> as 3 ev.

It would be very interesting to have better experimental results on the optical constants of lithium. Until now no experimental evidence has been found for the interband transitions in lithium. The optical matrix

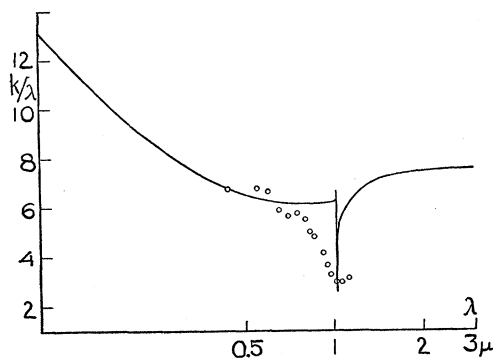


FIG. 11. The calculated values of  $k/\lambda$  vs  $\ln \lambda$  for zinc. The curve was computed with the Fermi surface having contact with the zone boundary. The value of  $a=0.0036$ ,  $\alpha=0.16$  and  $M=0.66$ . The circles denote the experimental points of Bor *et al.*<sup>36</sup>

<sup>37</sup> M. L. Glasser and J. Callaway, Phys. Rev. **109**, 1541 (1958).

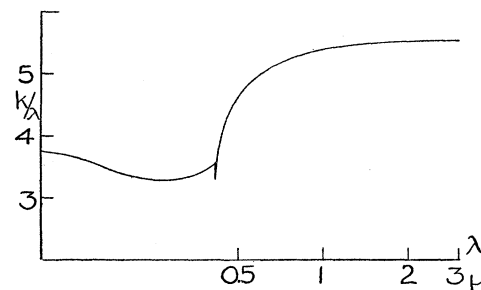


FIG. 12. The calculated values of  $k/\lambda$  vs  $\ln \lambda$  for lithium. The curve was computed with the Fermi surface having the contact with the zone boundary. The value of  $a=0.0001$ ,  $\alpha=0.25$  and  $M=0.22$ .

TABLE III. The Drude parameters adopted for the calculation of the dispersion curves for lithium and zinc. The energy gap assumed in the calculation of the interband contribution is given in electronvolts.

	$N$	$\sigma_0$	$m^*$	Energy gap
Lithium	4.8	1.05	1.37	3
Zinc	6.7	1.51	1	1.2

element for lithium should not be large in absolute value. The wavelengths, however, where deviations from the Drude theory are to be expected, lie in the visible which is more easily accessible for measurements.

In the course of the present investigation numerous tables of the dispersion curves have been computed for a wide variety of parameters. Copies can be obtained by interested persons.

#### ACKNOWLEDGMENTS

I should like to thank Professor H. Jones for suggesting this investigation, for many valuable discussions and for his very kind hospitality extended to me at the Imperial College.

I thank Professor W. Kohn and Professor J. Callaway for interesting discussions. I thank Mr. S. Michaelson for help in the programming. I am grateful to the London University Computer Unit for the allocation of the computer time. The maintenance grant of the Polish Academy of Science was held in the earlier, and an I.C. Fellowship in the later stage of this work.